JOURNAL OF MATERIALS SCIENCE 14 (1979) 1669–1675

# Indentation plasticity and microfracture in silicon carbide

JAMES LANKFORD, DAVID L. DAVIDSON
*Southwest Research Institute, San Antonio, Texas, USA*

The extent of the plastically deformed region associated with indentation in silicon carbide is determined by means of selected-area electron channelling. It is found that the extent of the plastic zone beneath an indent is quite large, i.e. equal to about five times the impression radius. Microcrack formation is studied in the SEM, and the combined results are discussed in terms of current elastic–plastic indentation fracture models. The first cracks to form are radial microcracks; their morphology, and the observed indentation plastic zone dimensions, support the elastic–plastic model of Perrott for indentation cracking in $\alpha$-SiC.

## 1. Introduction

Strong ceramics are utilized in situations in which they often are subject to wear or erosion. Many such service applications involve elastic–plastic indentation, i.e. indent (particle) radii are sufficiently small that some irreversible deformation is associated with the indentation process. The resulting subsurface plastic zone is involved in the "damage" of a specimen through its influence upon either microcrack initiation, or subsequent crack growth.

The specific role of indentation plasticity can be inferred from consideration of current theoretical treatments of the microfracture attending indentation in brittle materials. For example, the recent Lawn–Evans model [1] for crack initiation during elastic/plastic indentation is based upon the idea of the plastic zone "seeking out" and engulfing pre-existing subsurface crack nucleation centres, so that the plastic zone size becomes critical. Similarly, Perrott [2] has examined the possibility of near-surface radial cracking, and has developed a model whose correctness depends in large measure upon the physical realism of the analytical calculation of the static and residual plastic zone boundary. Finally, Evans and Wilshaw [3] have considered indentation crack propagation using fracture mechanics and dimensional analysis concepts. In this particular case the associated elastic analysis of indentation stresses for uniformly distributed contact pressure predicts that the first cracks to form should be median vents, and that the profile of the fractures should be a crescent surrounding the plastic zone and intercepting the surface. The results of the present study will be examined and interpreted from the viewpoint of these theories.

Several approaches, including X-ray diffraction, dislocation etch pitting, transmission electron microscopy (TEM), and selected-area electron channelling, have been used to study damage zones in metals and ceramics. Of particular relevance to the present study are the TEM studies by Hockey and co-workers [4–6], of indentation damage in ceramics, and the electron channelling characterization, by Ruff [7, 8], of sliding contact plastic zones in metals. In the former work, simple indentation techniques and particle impact at moderate velocity were used to produce indentation and microfracture in hard ceramics such as $Al_2O_3$ and SiC. The damage sites were sectioned for TEM study and the nature of the plastic deformation determined; to a lesser extent, some idea of the spacial extent of the damage zone, especially near the surface, was obtained. On the other hand, Ruff used electron channelling to characterize the extent of the plastic zones, and the strain distributions within them, for pure metals such as copper and iron subject to sliding contact. Here there was the advantage of working with bulk

0022–2461/79/071669–07 $2.70/0  

samples, so that the boundary of the subsurface damage zone relative to the sliding contact could be accurately mapped. In the present case, the electron channelling approach is applied to the study of quasi-static indentation in SiC, with the principal goal of determining the extent of plastic deformation beneath a sharp indenter. A second objective is to relate observed indentation microfracture patterns to the plastic zone.

## 2. Experimental procedure

A silicon carbide single crystal* ($\alpha$-SiC, 4H polymorph) approximately 7 mm in cross-section x 1 mm thick, having the *c*-axis perpendicular to the large pair of faces, was used in the study. Diamond pyramid hardness indentations were introduced into the as-grown surface using a standard microhardness tester; the indenter was applied quasi-statically, the specimen remaining under load for a total of 18 sec.

The reason for choosing a single crystal was two-fold. First, it was desired to eliminate crystallographic effects caused by varying grain orientation. Second, the electron channelling approach requires a relatively flat, initially low dislocation density, reference surface for mapping our plastic zones. Both goals were achieved by applying indentations, at a variety of loads, in a straight line across the specimen, with their spacing adjusted so that the tips of adjoining radial cracks almost touched. The specimen was then broken in three-point bending, producing a fracture surface passing through the centre of each indent. Since the bulk of the surface was created by fast fracture, it was anticipated that this region should afford an excellent reference (minimal deformation) state, based on the TEM study of Hockey and Lawn [5], in which no dislocations were observed at the tips of arrested cracks in SiC. Orientation of the fracture surface was determined using an electron channelling pattern map (Appendix 1).

The extent of plasticity beneath the indentations was determined using the same approach which the writers previously applied to the study of fatigue crack tips in metal alloys, as described extensively elsewhere [9–11]. Briefly, numerous locations beneath, and adjacent to, an indentation are interrogated with the electron beam. Rather than rastering back and forth to produce the normal image, however, the beam is rocked through an angle of (in this study) $\sim 7^\circ$, producing a selected-area electron channelling pattern. For the electron optical system and conditions used, an area approximately 10 $\mu$m diameter was interrogated by the beam. Line acuity in the electron channelling pattern is reduced by dislocations introduced as the result of plastic deformation. The locus about the indent along which fine structure and higher order lines in the channelling patterns are observed to just begin to disappear is taken to be the plastic zone boundary. In metals, this locus corresponds to approximately 0.2% tensile strain, based on tensile calibration specimens.

## 3. Results

Two basic types of indentation microfracture patterns were revealed by the cleavage technique, the most common being typified by Fig. 1, where several lateral cracks are seen to be associated with the indent. In addition, the outline of the radial indentation crack (arrows) lying in the plane of the fracture can be seen where it joins with the main crack. Running from the indent to the edge of the crack outline is a ledge (L), implying that the radial crack actually was made up of two segments, which grew until they met at the ledge. No median crack is visible normal to the plane of the fracture; this observation characterized 80% of the indentations.

In a few cases, a second situation prevailed, as shown in Fig. 2. Here lateral cracks and a "ledge" can be seen as before, but in addition, there exists

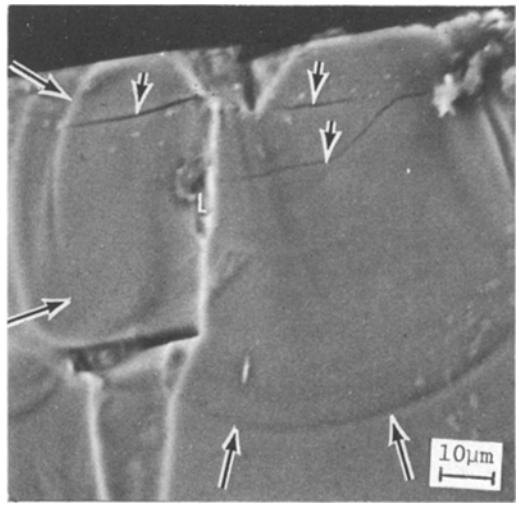


*Figure 1* Section through 3500 g indentation, showing lateral cracks (arrows), ledge (L), and outline of radial crack (arrows).

*Materials Research Corporation, Organgeburg, New York, USA.

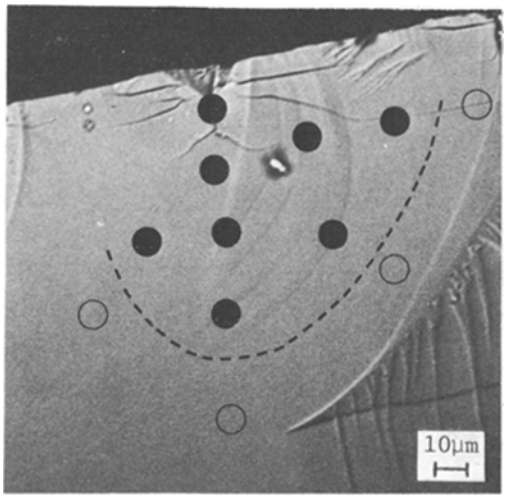


*Figure 2* Section through 1500 g indentation, showing lateral cracks, ledge, and short, branched median crack. Filled circles indicate locations of distorted ECPs, open circles locations in which no damage is seen. Dashed line outlines plastic zone boundary.

a branched median crack directly beneath the indent apex. It should be emphasized, however, that such cases were clearly in the minority, and that even for loads as high as 3500 g (which produced impression diameters and surface radial crack lengths of approximately 50 and 220 $\mu$m, respectively), subsurface median cracks usually were not seen. When they were present, the median cracks usually ran only a short distance, of the order of the indentation depth, before branching into lateral cracks. They were generally tightly closed near the indent.

Locations at which channelling patterns were taken are shown by the dots in Fig. 2, drawn to scale to indicate the approximate 10 $\mu$m interrogated area. Solid dots indicate channelling patterns degraded in quality by plastic flow, while open dots indicate undeformed ECPs. Fig. 3 shows channelling patterns obtained from locations lying (a) within, (b) just outside, and (c) far from the plastic zone boundary sketched in Fig. 2. It can be seen that Fig. 3b and c are essentially identical, while the pattern obtained from within the plastic zone shows a marked deterioration in quality.

Although the patterns in Fig. 3b and c are good, they are, in fact, not perfect. Comparison of these patterns with one taken from the virgin, as-grown surface of the crystal (Fig. 3d) shows that the latter is considerably sharper and richer in detail, implying that there may have been a slight amount of plastic deformation associated with passage of the main crack front. Fig. 3d does not, incidentally, show the six-fold symmetry one normally associates with a (0001) pole, because the surface was purposely tilted slightly away from 90° incidence with the beam so as to produce a channelling pattern more visually compatible with the others shown in Fig. 3.

Results of the plasticity measurements can be summarized generally in terms of maximum plastic zone depth, $R_y$, indentation diameter $2a$, and radial crack length $2c$, as shown in Fig. 4. Since the specimen is a single crystal, experimental scatter in these parameters is minimal. Inclusion of the indentation diameter in $c$ is somewhat arbitrary, since close SEM inspection of indentations shows (Fig. 5) that the radial cracks may not penetrate the interior of the indent; if they in fact do so, they are extremely tight cracks indeed.

From Fig. 4, it is evident that both $a$ and $c$ have a linear relationship with $R_y$; the situation with regard to $a$ can be expressed by

$$a = 0.18R_y. \quad (1)$$

Impressions were observed for loads as small as 2 g, for which $a = 0.6\,\mu$m, corresponding to an extrapolated plastic zone depth of 3.3 $\mu$m. Since the load $P$ is known to be proportional to $a^2$, it follows from Equation 1 that it also is proportional to $R_y^2$, as predicted by theory [2, 3]. The crack dimension $c$ requires a more complicated expression of the form

$$c = c^* + b(R_y - R^*), \quad (2)$$

where $c^*$ is the hypothetical minimum (threshold) crack size, $R^*$ is the indentation plastic zone size at the hypothetical threshold for crack initiation, and $b$ is a constant. Evaluation of these terms yields $c^* = 6\,\mu$m, $R^* = 34\,\mu$m, and $b = 0.95$. However, as it happens, the physical threshold for crack initiation can be determined to lie above that related to the point of intersection of the extrapolated $a$, $c$ versus $R_y$ plots. As will be reported in detail in a subsequent paper, scanning electron microscopy and acoustic emission show that the earliest cracks to form are radial cracks about 18 $\mu$m in length, corresponding to a critical plastic zone dimension $R_y \sim 50\,\mu$m. It is clear that at the time of crack initiation, the region below the indentation is essentially plastic. This is, in fact, true of the bulk of the material surrounding the impression, as shown in Fig. 6. Here are summarized the results (shaded band) of channelling

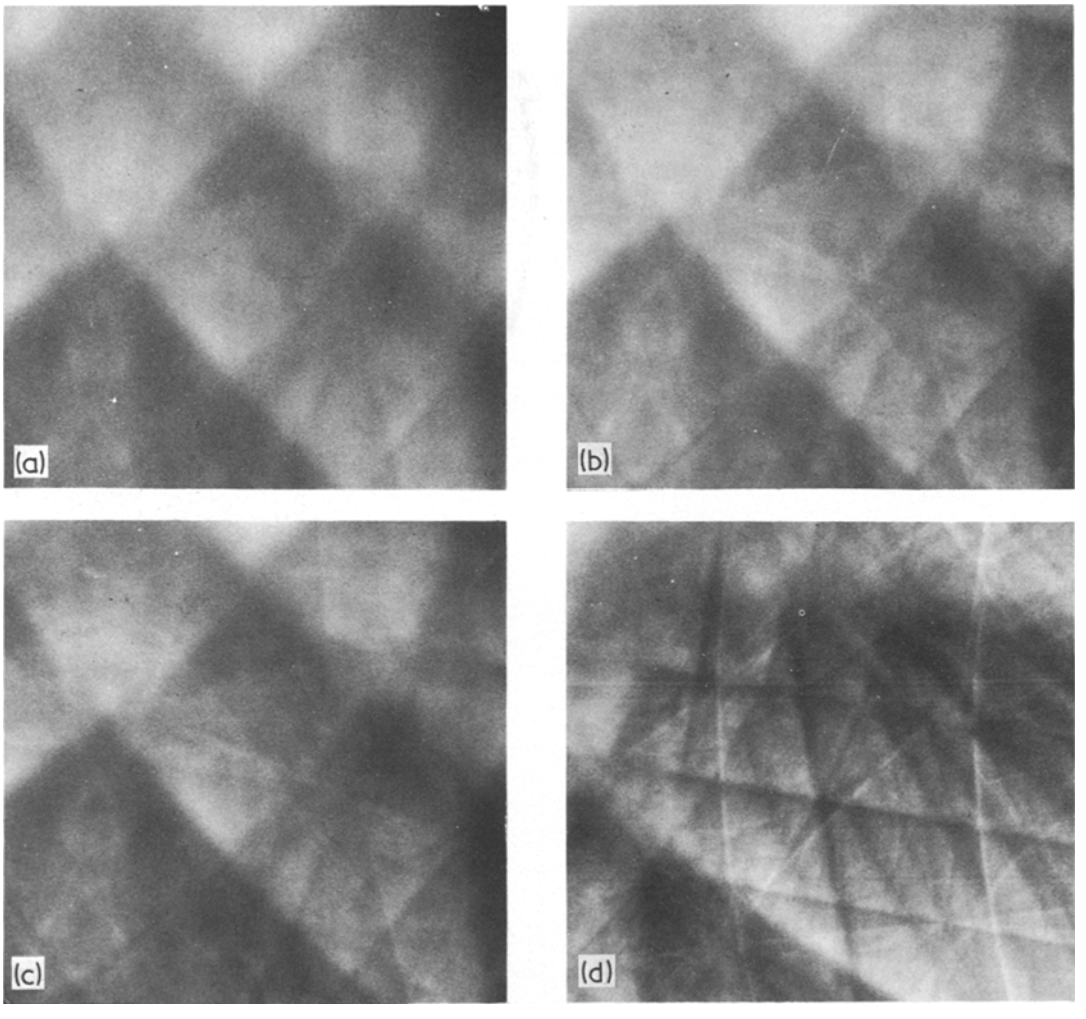


*Figure 3* Subsurface electron channelling patterns. (a) ECP within plastic zone. (b) ECP just outside plastic zone. (c) ECP far from plastic zone boundary. (d) ECP from as-grown (0001) face.

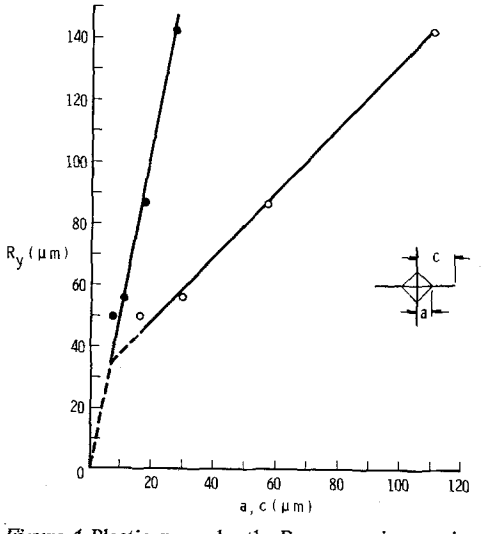


*Figure 4* Plastic zone depth, $R_y$, versus impressions radius and crack half-length for α-SiC; load range 200 to 350 g.

pattern measurements sampling various locations beneath the indentation, for loads between 200 and 3500 g. The notation used is similar to that of Perrott [2], whose calcuation of the plastic zone boundary ($\rho = \rho'$) following unloading of an indentation is shown in Fig. 7, with the normalized surface plastic zone radius chosen to be 4.0. For the particular theoretical case shown, i.e. $\rho'' = 4.0$, there is excellent agreement between the theoretical and experimental subsurface zone dimensions, e.g. $\rho'_y$ = normalized depth of the plastic zone, and $\rho'_x$ = normalized maximum surface projection of the plastic zone boundary.

## 4. Discussion and implications

From the crack profiles revealed by the sectioning procedure, it appears that each radial indentation crack nucleates as two segments, touching the

indent corners and intersecting the surface; at higher stresses, the two cracks join beneath the surface, producing a connecting ledge. Median cracks do not seem to be involved in the early stages of crack development. These findings are in general accord with the observations of Evans and Wilshaw [3], who studied crack development in a variety of ceramics, but they argue against the physical model of Lawn and Evans [1], which is based upon the idea of the median cracks being first to appear (this may, however, be the case [1] in glass). In another paper, we will present results which show that despite this apparent inconsistency with regard to the sequence of microfracture events, the Lawn and Evans analysis is quite successful in ordering a wide range of ceramics with respect to initial crack sizes and to the indentation loads required to initiate microfracture.

The physical model which clearly seems most representative of the prevailing state of affairs is that of Perrott [2]. The critical factors in establishing the applicability of the model are (1) that considerable subsurface plasticity must be evident; (2) in order for the hoop stress in the near-surface region to achieve tensile character, the surface plastic zone must be sufficiently large, i.e. $\rho'' > 1.65$, and (3) the first cracks to form should be radial (Palmqvist). All of these criteria are met, assuming that the coincidence of the theoretical and experimental subsurface plastic zone dimensions (Figs. 6 and 7) implies that the surface plastic zones are also in reasonable agreement, i.e. that $\rho'' \approx 4.0$. This important point is supported by the near-surface TEM observations of Hockey *et al.* [6], in which $\rho''$ for SiC was estimated to be $\approx 3.0$. The basis for the good agreement here between theory and experiment apparently lies in the more realistic formulation of the stress analysis, whereby Perrott realized, and took into account, the role of the indentation plastic zone in controlling the magnitude of the contact pressure; this in turn led to an analytical result for indentation accommodation by displacement within the plastic zone, indicating divergence of the elastic solution towards a state of triaxial compression near the load axis, and towards a state of triaxial tension near the surface (Fig. 7). For well-developed plasticity ($\rho'' > 1.65$), the tensile stresses generated across radial planes in the near surface region (Fig. 7) were found to be of the order of the "yield" strength ($\approx$ hardness/3). On the other hand, the maximum tensile stress along the load axis occurs at the elastic–plastic boundary, and is equal to $Y(1-2\nu)/(7-2\nu) \approx Y/13$, where $Y$ is

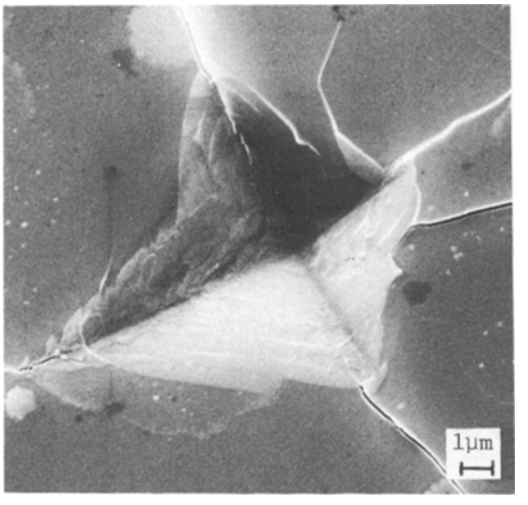


*Figure 5* Indentation, 250 g load, showing closure of radial cracks at edge of indent.

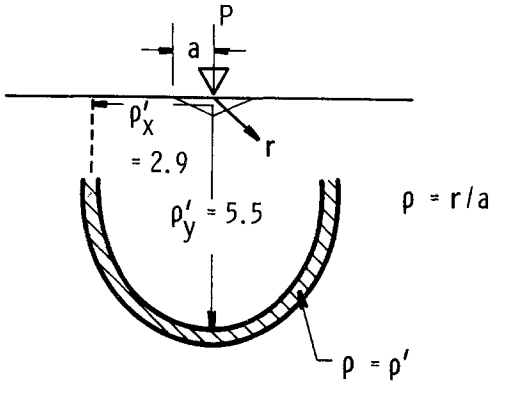


*Figure 6* Experimentally measured subsurface plastic zone in α-SiC, load range $P = 200$ to 3500 g.

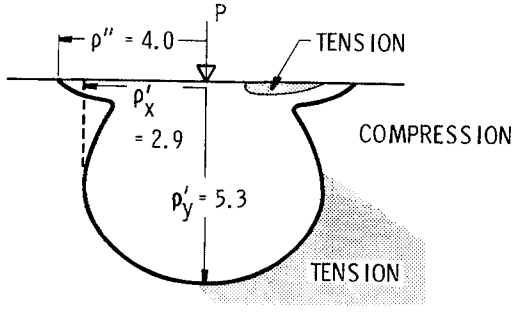


*Figure 7* Calculation [7] of plastic zone for elastic–plastic indentation following unloading of indent, $\rho'' = 4.0$; tensile regions are indicated by shading otherwise stresses are compressive.

the "yield" strength, and $\nu$ is Poisson's ratio. This factor for silicon carbide amounts to around 500 $MN\,m^{-2}$, which is just barely equal to the tensile strength of the material. Since this relatively low stress level "samples" only a very small volume of material for nucleating flaws, it is not surprising that tensile cracks are generated first in the near surface region, where the local hoop stress produces a tensile field thirteen times greater in magnitude than that along the load axis [2]. At higher loads, of course, there is a greater chance of generating median cracks below the plastic zone, since a larger material volume will be "sampled" by the plastic zone.

The threshold condition for crack initiation corresponds to a plastic zone depth of 50 $\mu$m, or apparently to a surface plastic zone dimension of about 35 $\mu$m ($\rho'' \approx 4.0$). Perrott [2] has shown analytically that tensile values of the hoop stress at the surface occur at radii $\rho$ less than 0.61 $\rho''$ adjacent to the boundary of the indentation. In the present case, this means that there exist regions extending nearly 9 $\mu$m out from the indentation corners, over most of which the local stress field is tensile, and considerably in excess of the tensile strength. From this, it is easy to see why the critical load for radial crack formation depends on the surface finish, decreasing as the quality of the surface diminishes [3].

The reduced sharpness of detail for channelling patterns obtained from the cleavage face in comparison with ones from the as-grown surface imply that some deformation was associated with passage of the main crack front. Hockey and Lawn [5], of course, reported an absence of dislocations near the tips of arrested indentation cracks in the same polymorph of SiC. However, the electron channelling phenomenon is extraordinarily sensitive to plastic damage, and there seems no other reasonable alternative to a dislocation-based explanation. It may be that the difference between the two experiments had to do with crack orientation rela-

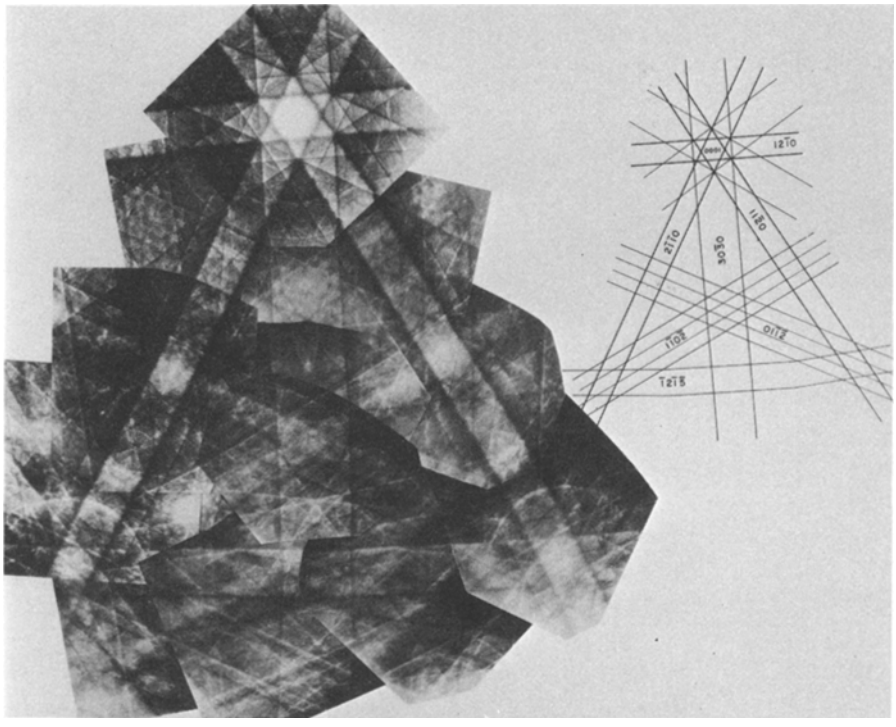


*Figure 8* Partial electron channelling pattern map, α-SiC, 30 keV.

tive to the specimen crystallography, although Hockey and Lawn examined foils from some two dozen indentations in SiC, which should have been a good statistical sampling. Nevertheless, other TEM work, on ($\beta$) SiC, does lend some support to this possibility. In this case, Clarke [12] examined areas immediately adjacent to the fracture surfaces of specimens broken in bending. It was found that in some grains, dislocations could be observed, depending on crystallography and, apparently, elastic constraint by other grains; in other grains, no dislocations were seen. Orientation of the crystal plane examined in the present experiment was approximately $(12\bar{3}0)$ (Fig. 8; see Appendix).

## 5. Conclusions

Indentations in $\alpha$-SiC exhibit considerable plasticity, with the depth of plastic damage extending to about five indent radii below the indentation. The measured plastic zone parameters and the observed fractography are compatible with the elastic–plastic analysis of Perrott, which predicts that the first (threshold) cracks to form, under conditions of sufficient plasticity, are radial rather than median cracks. This is in fact observed. It is found also that $a \propto R_y$, and $P \propto R_y^2$, in agreement with theory. The electron channelling results indicate that the fracture surfaces formed under conditions of rapid crack growth have experienced some plastic flow; this may turn out to be a crystallography-sensitive effect.

## Appendix

The polymorph and orientation of this material was determined using a partial channelling map, as shown in Fig. A1. This map was made from a single crystal having (0001) planes as the largest surfaces. Tilting of the crystal away from the (0001) causes the channelling line contrast reversal seen, for example along the $(\bar{1}2\bar{1}5)$ channelling band. By working out the hexagonal interplanar angles and comparing the derived unit cell dimensions with known values [1], the polymorph may be determined.


## Acknowledgement

The authors are grateful for the support of the Office of Naval Research, Contract no. N00014-75-C-0668, during the course of this work.


## References


1. B. R. LAWN and A. G. EVANS, *J. Mater. Sci.* **12** (1977) 2195.
2. C. M. PERROTT, *Wear* **45** (1977) 293.
3. A. G. EVANS and T. R. WILSHAW, *Acta Met.* **24** (1976) 939.
4. B. J. HOCKEY, *J. Amer. Ceram. Soc.* **54** (1971) 223.
5. B. J. HOCKEY and B. R. LAWN, *J. Mater. Sci.* **10** (1975) 1275.
6. B. J. HOCKEY, S. M. WEIDERHORN and H. JOHNSON, National Bureau of Standards Report, NBS1R 77-1396, December (1977).
7. A. W. RUFF, *Wear* **40** (1976) 59.
8. *Idem, ibid* **46** (1978) 251.
9. J. LANKFORD and D. L. DAVIDSON, *J. Eng. Mat. Tech.* **98** (1976) 17.
10. D. L. DAVIDSON and J. LANKFORD, *ibid* **98** (1976) 24.
11. J. LANKFORD, D. L. DAVIDSON and T. S. COOK, ASTM STP 637, American Society for Testing and Materials, Philadelphia (1977) p. 53.
12. D. R. CLARKE, "Proceedings Electron Microscopy Society of America", edited by G. W. Bailey (Claitor's, Baton Rouge, 1975) p. 64.
13. E. PARTHE, "Crystal Chemistry of Tetrahedral Structures" (Gordon and Breach, New York, 1965) p. 107.


Received 6 and accepted 13 October 1978.